Monatshefte für Chemie 125, 1171–1182 (1994)

Monatshefte für Chemie
Chemical Monthly

Synthesis and Properties of Iron(II) and Iron(III) Complexes with 3-(α,γ-Dicarboxy-*n*-propylidene-hydrazino)-5,6-diphenyl-1,2,4-triazine (*DCPT*)

A. A. T. Ramadan*, M. A. El-Behairy, A. I. Ismail, and **M. M. Mahmoud**

Department of Chemistry, Ain Shams University, Cairo, Egypt

Summary. Proton-ligand formation constants of *DCPT* and metal-ligand formation constants of its complexes with Fe(II) and Fe(III) have been determined potentiometrically at 10, 20, 30, and 40 °C in 75% (v/v) dioxane-water at 0.10 *M* ionic strength (KNO_3). The thermodynamic parameters ΔG, ΔH, and ΔS have also been evaluated. The possibility of forming $M(HL)$, $M(HL)_2$, and $M(HL)_3$ species was substantiated from potentiometric and electronic absorption measurements. The values of the stability constants $\log K_{M(HL)}$, $\log K_{M(HL)_2}$, and $\log K_{M(HL)_3}$ derived from the spectrophotometric method are in good agreement with those obtained from potentiometric data. The use of *DCPT* as an analytical reagent for the spectrophotometric determination of iron is discussed. The solid complexes have been characterized by chemical analysis and magnetic susceptibility, IR, NMR, and electronic spectral data.

Keywords. Iron complexes; *DCPT*.

Synthese und Eigenschaften von Eisen(II)- und Eisen(III)-Komplexen mit 3-(α,γ-Dicarboxy-*n*-propylidene-hydrazino)-5,6-diphenyl-1,2,4-triazin (*DCPT*)

Zusammenfassung. Die Bildungskonstanten sowohl von *DCPT* als auch seiner Komplexe mit Fe(II) und Fe(III) wurden bei 10, 20, 30 und 40 °C in Dioxan-Wasser (75% (v/v)) bei einer Ionenstärke von 0.1 *M* KNO_3 potentiometrisch bestimmt. Zusätzlich wurden die thermodynamischen Parameter ΔG, ΔH und ΔS ermittelt. Die Wahrscheinlichkeit des Auftretens von Komplexen der Art $M(HL)$, $M(HL)_2$ und $M(HL)_3$ wurde mittels potentiometrischer und absorptionsspektroskopischer Messungen erhärtet. Nach beiden Methoden ermittelte Stabilitätkonstanten stimmen gut überein. Die Verwendung von *DCPT* als analytisches Reagens zur spektrophotometrischen Eisenbestimmung wird diskutiert. Die Komplexe konnten in Substanz hergestellt werden und wurden durch chemische Analyse und über ihre magnetischen und spektroskopischen Eigenschaften charakterisiert.

Introduction

Previous investigations of the complexation of transition, post-transition, and lanthanoide elements by 3-(α-carboxymethyl-aminobenzylidene-hydrazino)-5,6-diphenyl-1,2,4-triazine (*HipHT*) [1] have shown that the higher negative enthalpy obtained for all complex systems is mainly due to the participation of the nitrogen atoms of –NH and –C=N in chelation in addition to the carboxylate oxygen atom.

To examine the effects of nonbinding carboxylate groups on complexation, we have studied the complexation of iron by *DCPT*. In this ligand, steric effects prevent simultaneous binding to both carboxylate sites. Potentiometry was used to obtain the thermodynamic parameters of complexation.

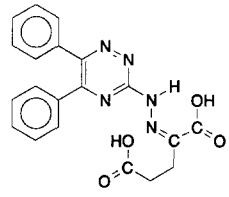

DCPT

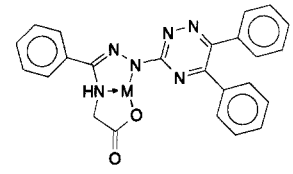

HipHT

Results and Discussion

Potentiometric measurements

The titration curves for the free ligand and complexed *DCPT* are shown in Fig. 1. The graph of the free ligand shows two buffer regions. The first one is situated between $a = 0$ and $a = 1$ (a = number of moles of base added per mole of ligand), followed by a weak inflection point at $a = 1$ due to the complete neutralization of the first carboxylate group. The second buffer region is located between $a = 1$ and $a = 2$, followed by a strong inflection at $a = 2$ due to the dissociation of the second carboxylate proton. This suggests that the *DCPT* ligand is diprotic (H_2L). The diprotic nature of *DCPT* is further confirmed by the titration curves of the ligand in the presence of Fe(II) or Fe(III). The weak inflection point at $a = 1$ indicates that the dissociation constants of the two COOH groups are close to each other. The values of K_1^H and K_2^H were calculated from the potentiometric titration data by the

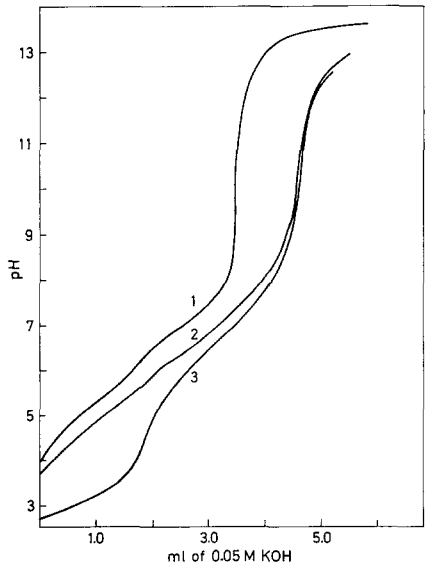

Fig. 1. Potentiometric titration curves for 30 ml of *DCPT* in absence and presence of metal ions ($T = 30\,°C$, $I = 0.1\,M$); 1: $[DCPT] = 0.003\,M$ 2: $1 + 0.001\,M$ Fe^{2+} 3: $1 + 0.001\,M$ Fe^{3+}

least-square method using the equation

$$\frac{\bar{n}_H}{(1-\bar{n}_H)\cdot[H^+]} = \frac{1}{K_2^H} + \frac{1}{K_1^H K_2^H}\frac{(2-\bar{n}_H)\cdot[H^+]}{(1-\bar{n}_H)}, \quad 1$$

where $\bar{n}_H$ is the average number of ionizable hydrogen atoms bound per ligand anion.

The *DCPT* curves obtained with 3:1 molar ratios of ligand to Fe(II) and Fe(III) are shown in Fig. 1. The shapes of these curves clearly indicate the formation of simple mononuclear chelates as well as various protonated species. The equilibria in the first buffer region may be represented by equations 2–7.

$$M^{z+} + HL^- \rightleftarrows M(HL)^{(z-1)+} \quad 2$$

$$K^M_{M(HL)} = [M(HL)^{(z-1)+}]/[M^{z+}][HL^-] \quad 3$$

$$M^{z+} + 2\,HL^- \rightleftarrows M(HL)_2^{(z-2)+} \quad 4$$

$$K^M_{M(HL)_2} = [M(HL)_2^{(z-2)+}]/[M^{z+}][HL^-]^2 \quad 5$$

$$M^{z+} + 3\,HL^- \rightleftarrows M(HL)_3^{(z-3)+} \quad 6$$

$$K^M_{M(HL)_3} = [M(HL)_3^{(z-3)+}]/[M^{z+}][HL^-]^3 \quad 7$$

Further addition of base results in the dissociation of three protons as indicated by the amount of base required per metal chelate. The reactions involved may be described by equilibria 8–19.

$$M^{z+} + L^{2-} + 2\,HL^- \rightleftarrows ML(HL)_2^{(z-4)+} \quad 8$$

$$K^M_{ML(HL)_2} = [ML(HL)_2^{(z-4)+}]/[M^{z+}][L^{2-}][HL^-]^2 \quad 9$$

$$M^{z+} + 2\,L^{2-} + HL^- \rightleftarrows ML_2(HL)^{(z-5)+} \quad 10$$

$$K^M_{ML_2}(HL) = [ML_2(HL)^{(z-5)+}]/[M^{z+}][L^{2-}]^2[HL^-] \quad 11$$

$$M^{z+} + 3\,L^{2-} + HL^- \rightleftarrows ML_3^{(z-6)+} \quad 12$$

$$K^M_{ML_3} = [ML_3^{(z-6)+}]/[M^{z+}][L^{2-}]^3 \quad 13$$

$$M(HL)_3^{(z-3)+} \rightleftarrows ML(HL)_2^{(z-4)+} + H^+ \quad 14$$

$$K^H_{ML(HL)_2} = [ML(HL)_2^{(z-4)+}][H^+]/[M(HL)_3^{(z-3)+}] \quad 15$$

$$ML(HL)_2^{(z-4)+} \rightleftarrows ML_2(HL)^{(z-5)+} + H^+ \quad 16$$

$$K^H_{ML_2}(HL) = [ML_2(HL)^{(z-5)+}][H^+]/[ML(HL)_2^{(z-4)+}] \quad 17$$

$$ML_2(HL)^{(z-5)+} \rightleftarrows ML_3^{(z-6)+} + H^+ \quad 18$$

$$K^H_{ML_3} = [ML_3^{(z-6)+}][H^+]/[ML_2(HL)^{(z-5)+}] \quad 19$$

Computer assisted algebraic methods were used to evaluate the three complex protonation constants present in the second buffer region. The results obtained together with the corresponding formation constants for $M(HL)^{(z-1)+}$, $M(HL)_2^{(z-2)+}$ and $M(HL)_3^{(z-3)+}$ at different temperatures are summarized in Table 1. The protonation constants of the free ligand at different temperatures are also included in Table 1.

Since iron(II) and iron(III) chelates have intense colours and absorb in the region 500–600 nm (Figs. 2 and 3), the formation constants of the protonated complexes have further been spectrophotometrically. In addition to the 1:1 complex which is

Table 1. Equilibrium constants and thermodynamic parameters for the interaction of *DCPT* and iron(II) and iron(III) ions ($I = 0.10\ M\ (KNO_3)$: 75% (v/v) dioxane-water.)

Symbol	Equilibrium quotient	ΔG, ΔH (k cal/mole); Fe(II)-*DCPT*			ΔS(cal/mole·K) Fe(III)-*DCPT*			$\log K^M$ Fe(II)-*DCPT*				Fe(III)-*DCPT*			
												10 °C	20 °C	30 °C	40 °C
		$-\Delta G$	$-\Delta H$	ΔS	$-\Delta G$	$-\Delta H$	ΔS	10 °C	20 °C	30 °C	40 °C				
$K^M_{M(HL)}$	$\frac{[M(HL)^{(z-1)+}]}{[M^{z+}][HL^-]}$	4.41 ± 0.02	3.26 ± 0.05	3.8 ± 0.06	6.84 ± 0.18	1.50 ± 0.01	17.6 ± 0.02	3.32	3.27	3.18 3.13*	3.08	6.01	4.97	4.93 5.22*	4.90
$K^M_{M(HL)_2}$	$\frac{[M(HL)_2^{(z-2)+}]}{[M^{z+}][HL^-]^2}$	4.30 ± 0.01	1.46 ± 0.01	9.4 ± 0.06	6.84 ± 0.18	1.34 ± 0.01	18.2 ± 0.03	3.18	3.13	3.10 3.06*	3.07	5.00	4.96	4.93 5.01*	4.90
$K^M_{M(HL)_3}$	$\frac{[M(HL)_3^{(z-3)+}]}{[M^{z+}][HL^-]^3}$	4.83 ± 0.14	−0.93 ± 0.01	19.0 ± 0.06	5.84 ± 0.11	3.27 ± 0.13	8.5 ± 0.34	3.43	3.46	3.48	3.50	4.56	4.40	4.35	4.31
$K^M_{ML(HL)_2}$	$\frac{[ML(HL)_2^{(z-4)+}]}{[M^{z+}][L^{2-}][HL^-]^2}$	4.36 ± 0.03	−5.33 ± 0.07	32.0 ± 0.30	5.49 ± 0.01	−0.81 ± 0.01	21.1 ± 0.01	2.82	3.00	3.14	3.21	3.92	3.94	3.96	3.99
$K^M_{ML_2(HL)}$	$\frac{[ML_2(HL)^{(z-5)+}]}{[M^{2+}][L^{2-}]^2[HL^-]}$	4.20 ± 0.38	−2.69 ± 0.04	22.7 ± 0.34	4.63 ± 0.17	−0.81 ± 0.01	18.0 ± 0.01	2.87	2.96	3.03	3.07	3.30	3.32	3.34	3.36
$K^M_{ML_3}$	$\frac{[ML_3^{(z-6)+}]}{[M^{z+}][L^{2-}]^3}$	4.72 ± 0.20	−1.62 ± 0.01	20.0 ± 0.01	4.83 ± 0.15	−1.62 ± 0.01	21.2 ± 0.01	3.39	3.36	3.40	3.44	3.40	3.44	3.48	3.52
								(log K^H)							
$K^H_{ML(HL)_2}$	$\frac{[ML(HL)_2^{(z-4)+}][H^+]}{[M(HL)_3^{(z-3)+}]}$	9.70 ± 0.08	16.56 ± 0.07	−22.6 ± 0.09	8.59 ± 0.03	6.62 ± 0.05	6.5 ± 0.05	7.89	7.35	6.99	6.65	6.43	6.20	6.19	5.93
$K^H_{ML_2(HL)}$	$\frac{[ML_2(HL)^{(z-5)+}][H^+]}{[ML(HL)_2^{(z-4)+}]}$	10.61 ± 0.14	18.90 ± 0.40	−27.4 ± 0.58	9.86 ± 0.09	6.14 ± 0.03	12.3 ± 0.06	8.79	8.03	7.65	7.37	7.43	7.22	7.11	6.90
$K^H_{ML_3}$	$\frac{[ML_3^{(z-6)+}][H^+]}{[ML_2(HL)^{(z-5)+}]}$	11.49 ± 0.14	18.64 ± 0.26	−23.6 ± 0.33	10.85 ± 0.13	7.36 ± 0.03	11.5 ± 0.04	9.38	8.69	8.28	7.99	8.17	7.96	7.82	7.61
K^H_1	$\frac{[HL^-][H^+]}{[H_2L]}$	7.13 ± 0.01	9.95 ± 0.02	−9.3 ± 0.02				5.63	5.41	5.14	4.90				
K^H_2	$\frac{[L^{2-}][H^+]}{[HL^-]}$	9.24 ± 0.01	5.88 ± 0.01	11.1 ± 0.01				6.98	6.82	6.66	6.55				

* spectrophotometric method

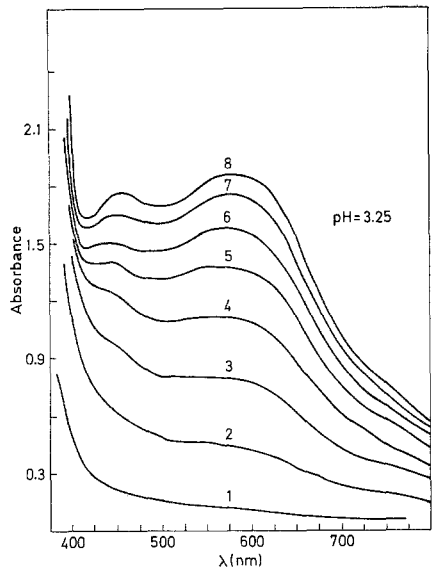

Fig. 2. Electronic absorption spectra of Fe^{2+}-*DCPT* chelates in 70% (v/v) dioxane-water; [Fe^{2+}]: 0.001 *M*; [*DCPT*]: 1, 0.0002 *M*; 2, 0.0006 *M*; 3, 0.0010 *M*; 4, 0.0014 *M*; 5, 0.0018 *M*; 6, 0.0022 *M*; 7, 0.0026 *M*; 8, 0.0030 *M*

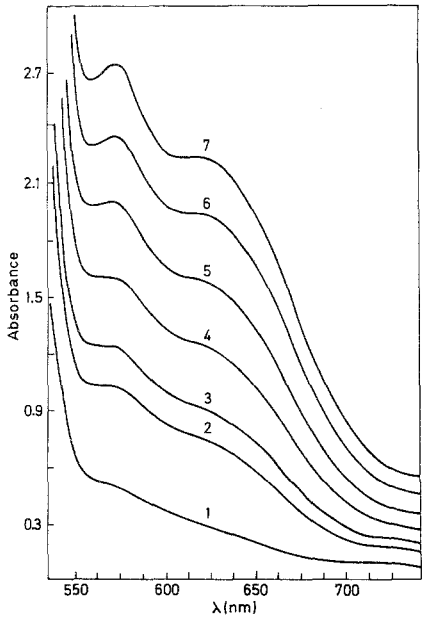

Fig. 3. Electronic absorption spectra of Fe^{3+}-*DCPT* chelates in 75% (v/v) dioxane-water; [Fe^{3+}]: 0.001 *M*; [*DCPT*]: 1, 0.0006 *M*; 2, 0.0010 *M*; 3, 0.0014 *M*; 4, 0.0018 *M*; 5, 0.0022 *M*; 6, 0.0026 *M*; 7, 0.0030 *M*

formed by the reaction

$$Fe^{z+} + H_2L \rightleftarrows M(HL)^{(z-1)+} + H^+ \qquad 20$$

at $pH < 5$, higher protic complex species ($Fe(HL)_2^{(z-2)+}$ and $Fe(HL)_3^{(z-3)+}$) may be produced with the increasing ligand concentration according to reactions 4 and 6. The successive formation constants K_n(n = 1, 2, and 3), expressed in terms of molar concentrations, are defined for each species by equations 3, 5, and 7. In the region of overlapping spectra of the free metal ion and its complex and assuming that only 1:1 complexes are formed ($C_L/C_M < 0.3$), relation 21 holds, where A and A_0 are the

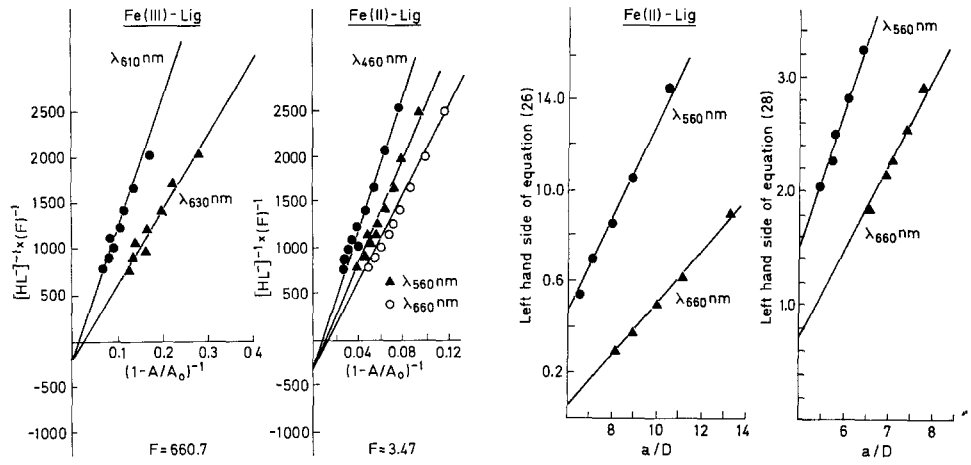

Fig. 4. Calculation of stability constants for Fe(II)-*DCPT* and Fe(III)-*DCPT* complexes by the Spectrophotometric method

absorbance in the presence and in the absence of *DCPT*, $\alpha = K^M_{M(HL)}\varepsilon_c/\varepsilon_m$ and ε_c and ε_m are the molar extinctions of the complex and the metal ion, respectively [4].

$$[HL^-]^{-1} = (1 - A/A_0)^{-1}(K^M_{M(HL)} - \alpha) - K^M_{M(HL)} \qquad 21$$

Plots of $[HL^-]^{-1}$ *vs.* $(1 - A/A_0)^{-1}$ give straight line whose intercept is $K^M_{M(HL)}$. The free ligand concentration has been calculated at any particular *pH* using equation 22.

$$c_{HL} = [HL^-](1 + K^H_1[H^+]) \qquad 22$$

A sample set of these calculations is presented in Fig. 4.

When the total concentration of ligand, *b*, is large with respect to the total metal concentration, a, two protonated species (1:1 and 1:2) are formed.

$$K^M_{M(HL)} = c_1/(a - c_1 - c_2)(b - c_1 - 2c_2) \qquad 23$$

$$K^M_{M(HL)_2} = c_2/c_1(b - c_1 - 2c_2) \qquad 24$$

c_2 represents the concentration of 1:2 complex. Since $b \gg a$, the above equations can be simplified, so that the absorbance is given by equation 25

$$D = \varepsilon_1 c_1 + \varepsilon_2 c_2 = \frac{a(\varepsilon_1 K^M_{M(HL)} b + \varepsilon_2 K^M_{M(HL)} K^M_{M(HL)_2} b^2)}{1 + K^M_{M(HL)} b + K^M_{M(HL)} K^M_{M(HL)_2} b^2}, \qquad 25$$

where ε_2 represents the molar extinction coefficient of the 1:2 complex. From equation 25 one obtains

$$\frac{1}{b^2 K^M_{M(HL)}} + \frac{1}{b} - \frac{a\varepsilon_1}{Db} = \frac{a}{D}\varepsilon_2 K^M_{M(HL)_2} - K^M_{M(HL)_2}. \qquad 26$$

The value of the left hand side of equation 26 was plotted against a/D. The values of ε_2 and $K^M_{M(HL)_2}$ were obtained from the slope and intercept of the straight line obtained (Fig. 4).

Taking into consideration the third species (1:3 complex), equations 27 and 28

are derived:

$$D = \frac{a(\varepsilon_1 K^M_{M(HL)} b + \varepsilon_2 K^M_{M(HL)} K^M_{M(HL)_2} b^2 + \varepsilon_3 K^M_{M(HL)} K^M_{M(HL)_2} K^M_{M(HL)_3} b^3}{1 + K^M_{M(HL)} b + K^M_{M(HL)} K^M_{M(HL)_2} b^2 + K^M_{M(HL)} K^M_{M(HL)_2} K^M_{M(HL)_3} b^3} \quad 27$$

$$\frac{1}{b^3 K^M_{M(HL)} K^M_{M(HL)_2}} + \frac{1}{b^2 K^M_{M(HL)_2}} - \frac{1}{b} - \frac{a\varepsilon_1}{Db K^M_{M(HL)_2}} - \frac{a\varepsilon_2}{Db} = \frac{a}{D}\varepsilon_3 K^M_{M(HL)_3} - K^M_{M(HL)_3} \quad 28$$

The left hand side of equation 28 was plotted against a/D, yielding the values of ε_3 and $K^M_{M(HL)_3}$ from the slope and intercept of the straight line obtained (Fig. 4). The values of the constants are in good agreement with the corresponding values obtained by the potentiometric method. The thermodynamic parameters ΔG, ΔH, and ΔS were calculated as described earlier (5). The values obtained are given in Table 2.

Spectral results

The absorption characteristics of the free ligand resemble basically these of triazine compounds. The spectrum in 75% (v/v) dioxane-water shows two absorption bands with $\lambda_{max} = 220$ and 292 nm and molar absorptivities of 6.0×10^4 and 1.2×10^5 l·mol^{-1}·cm^{-1}, these two bands are attributed to the enhanced $\pi \rightarrow \pi^*$ transition (K-band) over the whole conjugated systems and an enhanced $n \rightarrow \pi^*$ transition (R-band), respectively.

Upon mixing a solution containing Fe(II) and Fe(III) ions with a solution of *DCPT* in 75% (v/v) dioxane-water, coloured complexes are formed. At constant metal ion concentration (Fe^{2+} or Fe^{3+}) and varying ligand concentration, the absorbance increases rapidly at low concentrations of ligand but tends to attain a limiting value at higher concentrations (Figs. 2 and 3). Multiple band spectra indicate the probable formation of complexes with varying stoichiometry. The intensities of the peaks observed are functions of both the *pH* of the medium and the molar ratio of metal to ligand. In the case of Fe(II) and Fe(III) complexes, a maximum is reached at an *M*:*L* molar ratio of 1:3 (Figs. 2 and 3). As can be seen from Fig. 5, the absorbance has a maximum in the *pH* region 4.5–5.5, followed by a plateau in the *pH* region 6.0–8.5 for the Fe(II)-*DCPT* system. In the case of Fe(III)-*DCPT*, the absorbance shows a rapid increase in the *pH* region 2.0–4.0. From the absorbance *vs. pH* diagrams it can be concluded that the optimum *pH* values are 5.0 and 3.5 for the formation of Fe(II)-*DCPT* and Fe(III)-*DCPT* complexes, respecitively. In addition to the *pH*-absorbance plots, the curves for α_{MHL}, $\alpha_{M(HL)_2}$, $\alpha_{M(HL)_3}$, $\alpha_{ML(HL)_2}$, $\alpha_{ML_2(HL)}$, and α_{ML_3} (calculated from potentiometric data) are shown as a function of the *pH* of the solution (Fig. 6). A comparison of the plots shows that at $pH > 5.8$ and 5.0 for Fe(II)- and Fe(III)-*DCPT* systems, respectively, the absorbance is nearly constant (Fig. 4), indicating that both the protonated ($ML(HL_2)_2$ and $ML_2(HL)$) and nonprotonated (ML_3) species are absorbing to the same extent ($\varepsilon_{ML(HL)_2} = \varepsilon_{ML_3}$). The presence of two absorbing species in this *pH* region was substantiatd by applying *Coleman*'s graphical method [6] at different relevant pH-values. Typical plots are given in Fig. 7. The analysis revealed that only one absorbing species exists in the acidic region (below *pH* 5.8 and 5.0 for Fe(II) and

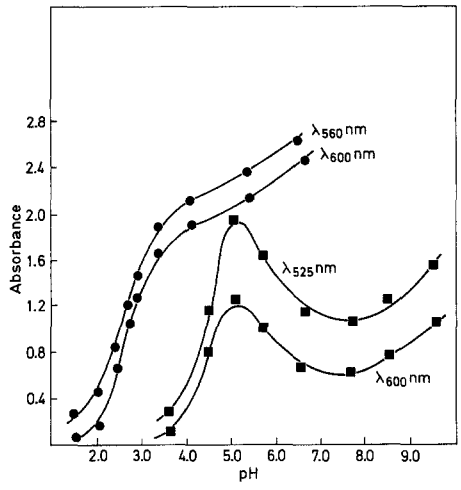

Fig. 5. Absorption *vs. pH* plots for Fe^{2+}-*DCPT* and Fe^{3+}-*DCPT* chelates; $[DCPT] = 0.003\ M$; $I = 0.10\ M$ (KNO_3); ■: Fe^{3+}: *DCPT* = 1:3; ●: Fe^{2+}: *DCPT* = 1:3

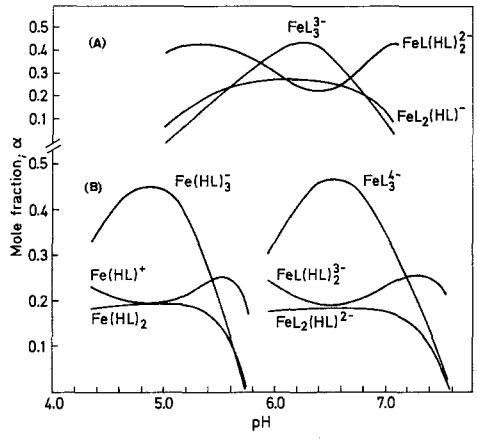

Fig. 6. Mole fraction *vs. pH* plots for (A) Fe(III)-*DCPT* and (B) Fe(II)-*DCPT* systems

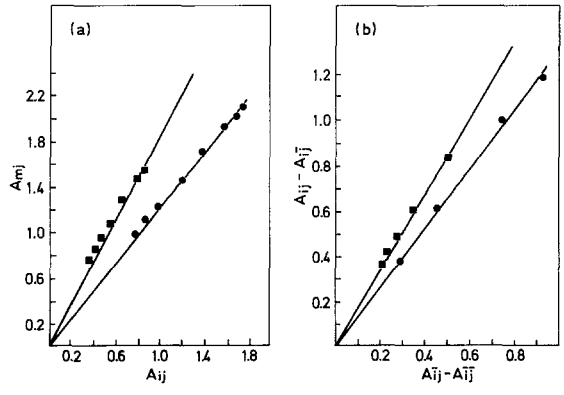

Fig. 7. *Coleman et al.*-plots for the different Fe(II)-*DCPT* chelates; (a) $pH = 2.18 - 4.50$; (b) *pH*: 5.13–7.50

Fe(III) chelates, respectively), which probably is that formed between metal ions and acidic ligands (Fig. 7a). Above *pH* 5.8 and 5.0 for Fe(II) and Fe(III) systems, respectively, two absorbing species (protonated and nonprotonated) were found as was indicated by the linear plots shown in Fig. 7b.

At constant ligand concentration and varying metal ion concentration, the absorbance increases steadily. The absorbance *vs.* c_{Fe}^{2+} and absorbance *vs.* c_{Fe}^{2+}

plots are linear; *Beer*'s law is valid within a certain concentration range ($2.5 \times 10^{-5} - 2.5 \times 10^{-4}\,M$ and $2.5 \times 10^{-4} - 2.5 \times 10^{-3}\,M$ for Fe(II) and Fe(III) ions, respectively). These limits together with the ε_{max} values (ε_{max} at 550 nm equals $1.1 \times 10^3\,l \cdot mol^{-1} \cdot cm^{-1}$ for the Fe^{3+} complex) indicate that *DCPT* can be readily utilized for micro-determination of iron(III). The molar absorptivity of iron(II)-*DCPT* complexes is considerably high ($1.3 \times 10^4\,l \cdot mol^{-1} \cdot cm^{-1}$). This fact further confirms that *DCPT* is a sensitive iron reagent, although it seems to contradict the emperical rule that phenyl substituents (such as the 5,6-diphenyl groups in *DCPT*) tend to decrease coplanarity and therefore π-electron delocalization.

The stiochiometries of the complexes were evaluated using slope ratios and continuous variation methods. The results proved that Fe(II) and Fe(III) form complexes with stiochiometric ratios of 1:1, 1:2 and 1:3 as a already indicated by our potentiometric investigations.

The magnetic data of the complexes are given in Table 1. The moments obtained for the Fe(II) and Fe(III) complexes with *DCPT* indicate that they are of a spin free octahedral type. However, the low moment associated with Fe(II)-*DCPT* might be attributed to a distortion from the octahedral structure with considerable π-bonding [7].

The high-spin iron(III) complexes contain five unpaired electrons; all d-d transitions are spin forbidden and hence should be weak. A pattern of four bands is usually expected for octahedral geometry corresponding to the transitions $^4T_{1g} \leftarrow {}^6A_{1g}$, $^4T_{2g} \leftarrow {}^6A_{1g}$, $^4E_g \leftarrow {}^6A_{1g}$, and $^4T_{1g}(D) \leftarrow {}^6A_{1g}$ [8]. However, not all transitions are observed in most of the complexes. The Fe(III)-*DCPT* complexes reveal two bands (562.5 and 625 nm) assignable to one of the transitions given above.

High-spin octahedral complexes of Fe(II) have a 5d ground state term, split by the crystal field into a ground $^5T_{2g}$ and an excited ^5E_g term [9]. A magnetic moment of 5.5 B.M. (*i.e.* 4.90 B.M. + orbital contribution) is expected for pure octahedral symmetry. We found a μ_{eff} of 4.80 B.M. for the Fe(II)-*DCPT* complex, obviously due to a distortion of the octahedral geometry. Similarly, in the electronic spectrum, the expected single band due to $^5E_g(t_{2g}^3 e_g^3) \leftarrow {}^5T_{2g}(t_{2g}^4 e_g^2)$ is broadened or split. Beside stereochemical distortions, spin-orbit coupling and a *Jahn-Teller* effect in the excited configuration contribute to band broadening. The band is found between 875.0–750 nm, apart from the two charge-transfer bands which are observed at 450 and 575 nm [10].

In the IR spectra of the ligand, strong broad bands at 3380 cm^{-1} and 3160 cm^{-1} can be assigned to ν_{OH} and ν_{NH}, respectively. A decrease of $\nu_{OH(strech)}$ can be attributed to hydrogen bonding. Instead of these two bands, one broad band at 3160–3400 cm^{-1} is observed in the spectra of the complexes due to the presence of coordinated water. The strong band at 1680 cm^{-1} in the *DCPT* spectrum is assigned to $\nu_{C=O(strech)}$ of the carboxylate groups. This band is shifted to 1610 cm^{-1} in Fe(III)-*DCPT* due to the participation of one of these carboxylate groups in chelate formation. In the case of Fe(II)-*DCPT*, this band disappears which indicates the participation of the two carboxylic groups in complex formation in accordance with the binuclear nature of this complex (Table 2). The non-ligand bands at 580 and 540 cm^{-1} could be assigned to ν_{M-O} and ν_{M-N}, respectively. The additional non-ligand band at 620 cm^{-1} in the case of Fe(II)-*DCPT* is due to ν_{M-O}- which arises from the participation of the second carboxylate group in the binuclear complex.

Further evidence for the coordination of the two carboxylate groups to the Fe(II) ion is confirmed from the proton NMR spectra for *DCPT* and its Fe(II) complex. The ^{1}H NMR spectrum (*DMSO*-d_6) of *DCPT* exhibits signals at 3.4 (m, 4H, $-CH_2-CH_2-$), 7.5 (m, 11H, reduced to 10H after D_2O exchange, N–H and aromatic protons), and 13.00 ppm (s, 2H, carboxyl groups). In the ^{1}H NMR spectrum of Fe(II)-*DCPT*, the signals for both carboxylic protons vanish, clearly confirming the complexatin of the ligand with Fe(II) after deprotonation.

It is known that iron ions (Fe^{2+} and Fe^{3+}) exist in solution as octahedrically hydrated species and the enthalpy (ΔH) values reflect the changes in the number and strength of bonds made and broken during the process of coordination. For Fe(II)-*DCPT* complexes, $\Delta H_{M(HL)}$ is more exothermic than $\Delta H_{M(HL)_2}$, while $\Delta H_{M(HL)_3}$ is endothermic. The values of the enthalpy with regard to the first, the second and the third reaction step can be rationalized by considering two processes: *a*) the displacement of one water molecule from the cationic coordination sphere by the carboxylate group of the ligand and *b*) the destructive process of the solvent as a consequence of the association of two charged particles. However, the crystal fields produced by oxygen coordinating ligands are similar to those of water molecule [11]; thus, ΔH will not be much affected by the displacement of water molecules by the carboxylate group of *DCPT*. In contrary, both above processes should contribute in a positive sense to ΔS values. Hence, the negative enthalpy values obtained for the first, second, and, in the case of the Fe^{3+}-*DCPT* system, third protonated complexes indicate that Fe(III) and Fe(II) interact with the nitrogen atom in the *DCPT* ligand.

The entropy of a simple hydrated ion is determined by its charge and radius, while the entropies of complex ions experience an additional contribution arising from structural factors [12]. The similarity in structure of the individual complexes of Fe(II) and Fe(III) ions causes the predominance of charge and radius as factors which govern the entropy change. Generally, the values of ΔS decrease as the radius of the cation increases, while for the enthalpy the general tendency is to become more exothermal for the hydrated ion and the complex as the metal ion radius decreases. This could explain why $Fe^{II}(HL)$ and $Fe^{II}(HL)_2$ complexes have lower entropy values than the corresponding $Fe^{III}(HL)$ and $Fe^{III}(HL)_2$ species.

The entropy value of $[Fe^{II}(HL)_3]^-$ is higher than that of $Fe^{III}(HL)_3$ by 10 cal/mol·K (Table 1). This difference could arise from the presence of the negative charge at the first complex while the second species is neutral. This explanation is supported by the presence of nearly the same difference in entropy (9.0 cal/mol·K) between the neutral complex $Fe^{II}(HL)_2$ and the charged compound $[Fe^{III}(HL)_2]^+$.

The enthalpy and entropy terms of complex formation reflect the disruption of solvent structures as well as the combination of the ions. The disruption of hydration structure (positive entropy) is an endothermic contribution while ion combination is an exothermic one. This perhaps could explain the positive entropy and negative enthalpy changes for the formation of $Fe^{II}(HL)$, $Fe^{III}(HL)$, $Fe^{II}(HL)_2$, $Fe^{III}(HL)_2$, and $Fe^{III}(HL)_3$.

The enthalpy changes for the dissociation of the first, second and third proton of the complexes $[Fe^{II}L(HL)_2]^{2-}$, $[Fe^{II}L_2(HL)]^{3-}$, and $[Fe^{II}L_3]^{4-}$ are rather similar (-16.6, -18.9, and -18.6 kcal/mol, respectively). The same trend can be observed for the corresponding Fe(III) complexes species (Table 1). This behaviour can be

explained on the basis that in these dissociation processes neutralization of the second carboxylate group takes place. The lower values of the entropy change (−22.6, −27.4, and −23.6 kcal/mol) obtained for the dissociation of the protons in the complexes $Fe^{II}L(HL)_2$, $Fe^{II}L_2(HL)$, and $Fe^{II}L_3$, respectively, indicate that no disruption of the hydration sphere occurs. This agrees well with the nature of the neutralization process of the second carboxylate group in which the enthalpy change is the driving force.

Experimental

Preparation of the solid ligand and its iron complexes

A mixture of 3-hydrazino-5,6-diphenyl-1,2,4-triazine (**1**) (0.01 mol) and ∝-oxo-glutaric acid in absolute ethyl alcohol (50 ml) was refluxed for 15 min and left standing overnight. The solid compound was obtained by dilution with cold water. The resultant solid was filtered and crystallized from ethanol to give 3-(α,γ-dicarboxy-*n*-propylidenehydrazino)-5,6-diphenyl-1,2,4-triazine (*DCPT*). The elemental analysis data for C, H, and N are presented in Table 2.

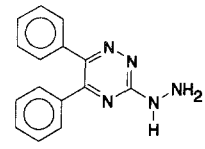

1

The iron(III) chelate was prepared by adding a dioxane solution of a *DCPT*(0.02 mol) to an aqueous solution of ferric nitrate (0.02 mol). The mixture was refluxed for 1 h. The red solid obtained was filtered off, washed with aqueous dioxane and dried under vacuum. A similar Procedures was followed in the case of the Fe(II)-*DCPT* complex except that the mixture was kept under a purified nitrogen atmosphere overnight in the course of which a violet solid gradually separated. The elemental analysis results for C, H, N, and Fe are given in Table 2.

Reagents, materials and procedures

For starting materials, purification of solvents and procedures see Ref. [2]. Conductance and magnetic moment measurements as well as recording parameters for infrared, UV-visible, and ^1H NMR spectra are described in Lit. [2, 3].

Table 2. Analytical data for *DCPT* and its iron complexes

Species and formula	%C Calc. (Found)	%H Calc. (Found)	%N Calc. (Found)	%Fe Calc. (Found)	Conductance ($ohm^{-1}\cdot cm^2\cdot mol$)	μ_{eff} (B.M.)
DCPT $(C_{20}H_{17}N_5O_4)\cdot H_2O$	58.68 (58.96)	4.65 (4.68)	17.12 (17.00)			
$[Fe(C_{20}H_{15}N_5O_4)(H_2O)_3]NO_3$	42.79 (43.20)	3.74 (4.30)	15.14 (15.00)	10.07 (10.00)	66.0	6.13
$[Fe_2(C_{20}H_{15}N_5O_4)(OH)(H_2O)_8]$	36.27 (36.84)	4.84 (4.74)	10.58 (10.38)	16.88 (16.30)	12.0	4.80

References

[1] Ramadan A. A. T., Abdel-Rahman R. M., El-Behairy M. A., Ismail A. I., Mahmoud M. M. (1992) Thermochim. Acta **222**: 291
[2] Ramadan A. A. T. (1991) Thermochim. Acta **186**: 245
[3] Ramadan A. A. T., Seada M. H., El-Behairy M. A., Ismail A. I., Mahmoud M. M. (1992) Anal. Letters **26**: 745
[4] Nach C. P. (1960) J. Phys. Chem. **64**: 950
[5] Ramadan A. A. T., Abdel-Moez M. S., Sleem H. S., El-Shetary B. A. (1992) Acta Chimica Hungarica – Models In Chemistry **129**: 619
[6] Coleman J. S., Varga L. P., Mastin S. H. (1970) Inorg. Chem. **9**: 1015
[7] Burman S., Stayamatayana J. (1982) Coord. Chem. **11**: 219
[8] Bertrand J. A., Eller P. G. (1974) Inorg. Chem. **13**: 927
[9] Greenwood N. N., Earnshow A. (1985) Chemistry of the elements. Pergamon Press, Oxford
[10] Jorgensen C. K. (1954) Acta Chem. Scand. **8**: 1502
[11] Nancollas G. H. (1966) Interactions in electrolytic solutions. Elsevier, Amsterdam
[12] Cobble J. W. (1953) J. Chem. Phys. **21**: 1451

Received February 23, 1993. Accepted March 10, 1993